ЭКОБИОТЕХ
ISSN 2618-964X http://ecobiotech-journal.ru
УДК 577.2/575.112

CC BY

RESEARCH ARTICLE | НАУЧНАЯ СТАТЬЯ

TRANSCRIPTOMIC SIGNATURES OF DOCETAXEL ADAPTATION IN THE PC3 PROSTATE CANCER CELL LINE: NF-κB/IL6/JAK/STAT3-SIGNALING AND CHOLESTEROL METABOLISM AS GUIDES FOR THE SEARCH FOR FUNGAL SECONDARY METABOLITES

Katunina I.V., Shishkina A.S., Pudova E.A.

Engelhardt Institute of Molecular Biology, Russian Academy of Sciences, Moscow, Russia
*E-mail: pudova_elena@inbox.ru

Abstract

Chemotherapy resistance remains a key contributor to the reduced effectiveness of cancer treatment. The aim of this study was to identify transcriptomic programs associated with the development of docetaxel adaptation in a PC3 cell model of prostate cancer and evaluate their applicability for the subsequent search for modifiers among fungal secondary metabolites. The experimental cells were exposed to docetaxel for prolonged periods, followed by selection of the surviving cell population. Using RNA-seq and GSEA analyses, we identified positive enrichment of the «TNFα signaling via NF-κB», inflammatory response, and «IL6/JAK/STAT3 signaling» pathways, which is consistent with the formation of an NF-κB/IL6/JAK/STAT3-associated survival signature. We also demonstrated the statistical significance of enrichment of the «Cholesterol homeostasis» pathway, suggesting the transcriptional remodeling of cholesterol-associated metabolic programs. The obtained data allow us to consider the identified transcriptomic programs as guidelines for subsequent targeted search and experimental testing of fungal secondary metabolites that are potentially capable of modifying inflammatory signaling and metabolic mechanisms of drug tolerance in tumor cells.

Keywords:

prostate cancer, chemotherapy, docetaxel, cell lines, transcriptome, fungal secondary metabolites

ТРАНСКРИПТОМНЫЕ СИГНАТУРЫ АДАПТАЦИИ К ДОЦЕТАКСЕЛУ В КЛЕТОЧНОЙ ЛИНИИ РАКА ПРЕДСТАТЕЛЬНОЙ ЖЕЛЕЗЫ PC3: NF-κB/IL6/JAK/STAT3-СИГНАЛИНГ И МЕТАБОЛИЗМ ХОЛЕСТЕРИНА КАК ОРИЕНТИРЫ ДЛЯ ПОИСКА ВТОРИЧНЫХ МЕТАБОЛИТОВ ГРИБОВ

Катунина И.В., Шишкина А.С., Пудова Е.А.

Институт молекулярной биологии им. В.А. Энгельгардта РАН, г. Москва, Россия
*E-mail: pudova_elena@inbox.ru

Аннотация

Химиорезистентность остается ключевым фактором снижения эффективности при лечении рака. Целью данного исследования была идентификация транскриптомных программ, связанных с развитием адаптации к доцетакселу на модели PC3 клеток рака предстательной железы, и оценка их применимости для последующего поиска модификаторов среди вторичных метаболитов грибов. Экспериментальные клетки подвергались воздействию доцетаксела в течение длительного времени, после чего проводилась селекция выжившей популяции клеток. С помощью RNA-seq и GSEA подходов нами было выявлено положительное обогащение сигнальных путей «TNFα signaling via NF-κB», воспалительного ответа и «IL6/JAK/STAT3 signaling», что указывает на активацию NF-κB/IL6/JAK/STAT3 сигнатуры выживания. Также нами была показана статистическая значимость обогащения пути «Cholesterol homeostasis», что указывает на транскрипционную перестройку метаболических программ, связанных с холестерином. Полученные данные позволяют рассматривать выявленные транскриптомные программы в качестве ориентиров для последующего целенаправленного поиска и экспериментального тестирования вторичных метаболитов грибов, потенциально способных модифицировать воспалительную сигнализацию и метаболические механизмы лекарственной устойчивости в опухолевых клетках.

Ключевые слова:

рак предстательной железы, химиотерапия, доцетаксел, клеточные линии, транскриптом, вторичные метаболиты грибов

Received: 19.05.2026
Accepted: 04.06.2026

Поступила в редакцию: 19.05.2026
Принято в печать: 04.06.2026

Cite as | Цитировать

DOI: http://doi.org/10.31163/2618-964X/2026-17 EDN: https://www.elibrary.ru/nmqllk

INTRODUCTION

Chemotherapy is a key approach in the treatment of various malignancies. However, despite its proven clinical efficacy, treatment outcomes are often limited by the development of resistance in many patients. Chemoresistance is characterized by a partial or complete loss of tumor cell sensitivity to cytostatic drugs during treatment and is one of the main causes of subsequent disease progression [Zafar *et al.* 2025]. Under conditions of chemotherapeutic stress from a cytostatic drug, tumor cells are capable of activating various adaptive mechanisms, such as cell cycle rearrangement, enhanced damage repair, metabolic reprogramming, activation of inflammatory signaling pathways, and many others [Gu *et al.* 2025]. These complex rearrangements contribute to the selection of surviving tumor cells with a phenotype of tolerance to the chemotherapeutic drug, and the study of these molecular programs is an important step in the development of strategies to improve the effectiveness of therapy [Dhiman *et al.* 2026].

High-throughput transcriptome sequencing (RNA-seq) combined with bioinformatics analysis provides a powerful tool for identifying molecular signatures of drug response. RNA-seq allows one to evaluate not only changes in the expression of individual genes but also coordinated changes in biological pathways and regulatory programs [Ergin *et al.* 2022]. When combined with functional enrichment methods, including Gene Set Enrichment Analysis (GSEA), this approach allows one to identify transcriptome signatures associated with cellular stress, inflammatory signaling, apoptosis, metabolic adaptation, and other processes potentially involved in the development of drug tolerance [Candia, Ferrucci 2024; Menyhart *et al.* 2025].

The use of transcriptome analysis followed by the selection of biologically active compounds directed at the identified targets represents a promising strategy for searching for candidate compounds that can potentially modify drug tolerance in tumor cells. In the context of the search for compounds capable of modifying the adaptive programs of tumor cells and increasing their sensitivity to therapy, fungal secondary metabolites are of particular interest. Fungi are a rich biotechnological source of structurally diverse bioactive compounds, including polyketides, terpenoids, alkaloids, peptidic and hybrid metabolites [Bills, Gloer 2016]. A number of such compounds can influence apoptosis, the cell cycle, inflammatory signaling, metabolic regulation, drug transport and tumor plasticity [Sonowal *et al.* 2024]. Of particular importance is the fact that the potential of the fungal metabolome remains far from fully explored. Fungi are characterized by the presence of numerous biosynthetic gene clusters, many of which are silent and can be activated through changes in cultivation conditions, epigenetic regulation or microbial interactions [Zhang *et al.* 2024]. It is also worth noting that less than 1% of the identified fungal biosynthetic clusters are associated with characterized compounds, which indicates a significant reserve for the search for new molecules with antitumor, anti-inflammatory and signal-modulatory activity [García-Estrada *et al.* 2025].

The aim of this study was to identify transcriptomic programs associated with the development of docetaxel adaptation in a cellular model of prostate cancer (PCa) – PC3. PCa is one of the most common malignancies in men worldwide, and advanced and castration-resistant PCa (CRPC), in which the tumor retains the ability to grow despite androgen suppression, poses a particular therapeutic challenge [Le *et al.* 2023; Siegel *et al.* 2025]. Docetaxel (DTX), a taxane-based chemotherapeutic agent, remains clinically important for these patients, since it became the first chemotherapeutic drug to demonstrate an overall survival benefit in metastatic CRPC [Hussain *et al.* 2024]. However, the efficacy of DTX may be reduced due to adaptation of tumor cells to repeated drug exposure. This adaptation does not necessarily indicate stable resistance, but may reflect the development of a state of drug tolerance, in which surviving cells activate compensatory survival programs [Sekino, Teishima 2020].

In this study, we generated a cellular model of PCa after repeated exposure to DTX to identify early transcriptomic programs of drug adaptation. Using RNA-seq and subsequent GSEA analysis, we identified biological pathways and regulatory programs associated with the adaptive response of PC3 cells to DTX. Additionally, the identified transcriptomic signatures were used to prioritize classes of fungal secondary metabolites potentially suitable for further targeted screening for modifiers of drug tolerance.

MATERIALS AND METHODS

PC3 cells were obtained from the American Type Culture Collection (ATCC) and cultured in RPMI-1640 medium supplemented with 10% FBS, L-glutamine, 100 U/mL penicillin, and 100 µg/mL streptomycin at 37°C in 5% CO_2. For cell dissociation, TrypLE™ Express Enzyme (Gibco, USA) was used. Cell counting was performed using the Countess II FL Automated Cell Counter (Thermo Fisher Scientific, USA). PC3 cells were seeded in 6-well plates at a density of 500,000 cells per well. DTX-selected PC3 cells were generated using a stepwise selection protocol that included three sequential rounds of treatment with increasing DTX concentrations (Sigma-Aldrich, USA): 4, 8, and 10 nM. At each round, cells were incubated for 24 h in complete culture medium containing the corresponding DTX concentration. After treatment, the DTX-containing medium was removed, and surviving cells were transferred to DTX-free complete medium for recovery. The next selection round was performed after the surviving adherent cells resumed proliferation and reached approximately 80% confluence. Cells that survived and recovered after the third round of treatment with 10 nM DTX were defined operationally as DTX-selected PC3 cells. Control PC3 cells were cultured in parallel under the same conditions and treated with an equivalent volume of DMSO without DTX exposure. Three biological replicates were included for each group. Mycoplasma contamination was assessed at each stage of the experiment using the MycoReport PCR-based detection kit (Evrogen, Russia) according to the manufacturer's instructions.

Total RNA was isolated from experimental cell samples using the RNeasy Micro Kit (Qiagen, Germany) according to the manufacturer's protocol. RNA concentration was estimated using the Qubit™ RNA BR Assay Kit (Thermo Fisher Scientific, USA) on a Qubit 4.0 fluorometer. The quality of the RNA was assessed using the Agilent RNA 6000 Nano Kit (Agilent Technologies, USA) on an Agilent 2100 Bioanalyzer. The RNA integrity number (RIN) was not lower than 9 for all samples.

Library preparation was performed using the KAPA RNA HyperPrep Kit with RiboErase (HMR or Human/Mouse/Rat) (Roche), according to the manufacturer's protocol. The final RNA-seq libraries quality was analyzed on an Agilent Bioanalyzer 2100 instrument (Agilent Technologies, USA) using the Agilent High Sensitivity DNA Kit (Agilent Technologies). The concentration of the libraries was measured on a Qubit 4.0 fluorometer (Thermo Fisher Scientific) using the Qubit dsDNA HS Assay Kit (Thermo Fisher Scientific). The final RNA-seq libraries were approximately 500 base pairs in length. Prepared mRNA libraries were combined into a single pool in equal proportions and subsequently diluted to a final concentration of 1 nM. Sequencing was performed on a NextSeq 2000 instrument using NextSeq 2000 P2 Reagent Kit (100 cycles) in single-end read mode. To minimize potential batch effects, all RNA-seq libraries were sequenced within a single sequencing run.

Primary processing of the resulting RNA-Seq data in FASTQ format was performed as described previously [Pudova *et al.* 2022]. The quality of raw FASTQ files was assessed using FastQC and MultiQC. Adapter sequences and low-quality reads were removed using Trimmomatic, followed by alignment to the human reference genome GRCh38 using the STAR aligner. Gene-level read counts were generated using featureCounts from the Subread package. Each sample yielded at least 10 million reads. For downstream analysis, the raw count matrix generated by featureCounts was imported into the R statistical environment. Differential gene expression analysis was performed in R using the DESeq2

package. Differentially expressed genes were identified using the Wald test for significance testing of log2 fold changes.The Benjamini–Hochberg correction was applied to calculate the false discovery rate (FDR). Differences in gene expression were considered statistically significant at an FDR < 0.05. Gene Set Enrichment Analysis (GSEA) was performed using the clusterProfiler package and Hallmark gene sets from the Molecular Signatures Database (MSigDB). For preranked GSEA, genes were ranked according to the DESeq2 Wald statistic obtained from the comparison between DTX-selected and control PC3 cells. Gene sets with an FDR < 0.05 were considered statistically significant. Variance-stabilized expression (VST) values generated with DESeq2 were used for visualization of selected genes in heatmaps.

Additionally, an external *in silico* analysis was performed to assess the concordance of the identified transcriptomic signatures at the pathway level. The analysis was carried out using two independent public RNA-seq datasets of PC3 cells after DTX treatment, GSE233647 and GSE140440, applying an approach analogous to that described above.

RESULTS

To identify biological processes associated with the development of DTX adaptation in PC3 cells, we performed Hallmark gene set enrichment analysis comparing DTX-selected PC3 cells with control cells. We identified 22 statisticq2ally significantly enriched signatures, including both positively and negatively enriched signatures/pathways (tab.1, fig.1).

Table 1. GSEA statistics for significantly enriched Hallmark signatures in DTX-selected PC3 cells compared with control cells

Таблица 1. GSEA статистика для значимых обогащённых Hallmark сигнатур в DTX-отобранных клетках PC3 по сравнению с контрольными клетками

Pathway	ES	NES	Gene set size	FDR
TNFα signaling via NF-κB	0.68	2.69	174	4.70×10^{-21}
Interferon gamma response	0.63	2.40	146	5.39×10^{-13}
Interferon alpha response	0.66	2.36	89	2.46×10^{-9}
p53 pathway	0.55	2.16	171	3.81×10^{-9}
Cholesterol homeostasis	0.62	2.12	69	5.97×10^{-6}
Hypoxia	0.50	1.91	154	1.79×10^{-5}
Apoptosis	0.48	1.82	128	1.14×10^{-4}
UV response up	0.47	1.76	129	3.91×10^{-4}
Inflammatory response	0.47	1.76	117	5.93×10^{-4}
Estrogen response early	0.43	1.67	162	6.15×10^{-4}
IL6/JAK/STAT3 signaling	0.59	1.91	51	1.32×10^{-3}
Oxidative phosphorylation	0.40	1.58	194	1.82×10^{-3}
Xenobiotic metabolism	0.43	1.66	136	1.87×10^{-3}
Complement	0.43	1.62	139	2.79×10^{-3}
Protein secretion	-0.48	-1.70	94	3.96×10^{-3}
Estrogen response late	0.41	1.57	149	3.96×10^{-3}
E2F targets	-0.39	-1.51	199	3.96×10^{-3}
Epithelial-mesenchymal transition	0.41	1.57	147	3.96×10^{-3}
Mitotic spindle	-0.40	-1.54	193	3.96×10^{-3}
Allograft rejection	0.45	1.61	97	4.10×10^{-3}
G2/M checkpoint	-0.38	-1.49	196	4.60×10^{-3}
Adipogenesis	0.37	1.44	171	1.48×10^{-2}

Note. ES, enrichment score; NES, normalized enrichment score; FDR, false discovery rate. Positive NES values indicate enrichment in DTX-selected PC3 cells, whereas negative NES values indicate negative enrichment relative to control PC3 cells. Gene set size indicates the number of genes from the corresponding Hallmark gene set included in the GSEA analysis.

Примечание. Столбчатые диаграммы показывают нормализованный показатель обогащения для каждого биологического процесса. Положительные значения NES соответствуют сигнатурам, обогащённым в DTX-отобранных клетках PC3, и показаны красным цветом; отрицательные значения NES соответствуют сигнатурам с отрицательным обогащением относительно контрольных клеток и показаны зелёным цветом.

Figure 1. Significantly enriched Hallmark signatures in DTX-selected PC3 cells compared with control cells

Рисунок 1. Значимые обогащённые Hallmark сигнатуры в DTX-отобранных клетках PC3 по сравнению с контрольными клетками

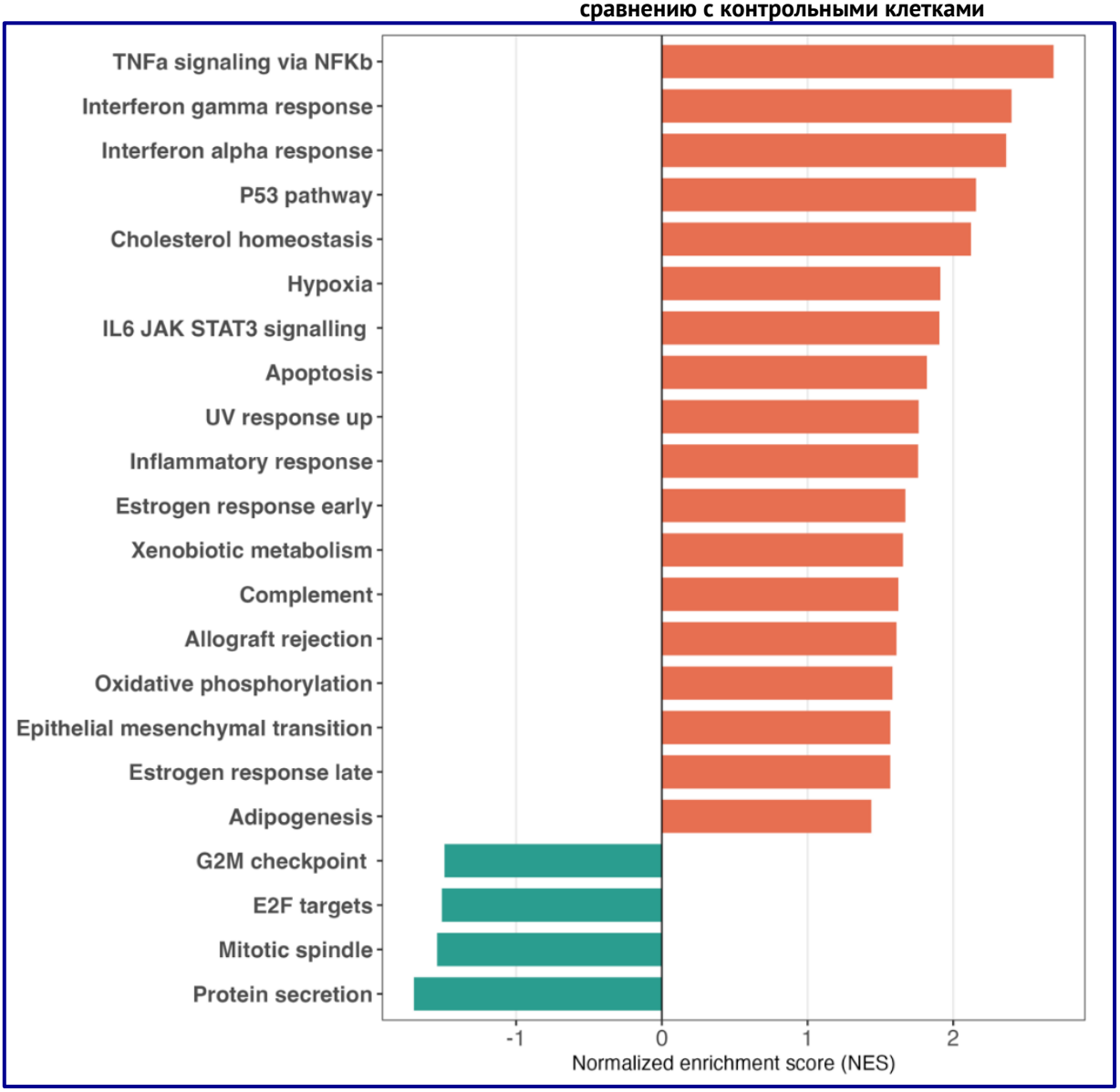

Note. Bar plots show the normalized enrichment score (NES) for each biological process. Positive NES values correspond to signatures enriched in DTX-selected PC3 cells and are shown in red; negative NES values correspond to signatures negatively enriched relative to control cells and are shown in green.

Примечание. Диаграмма Венна показывает перекрытие значимо обогащённых Hallmark сигнатур между тремя наборами данных. Тепловая карта показывает нормализованный показатель обогащения (NES) для этих общих путей. Красный цвет указывает на положительное обогащение, тогда как синий цвет указывает на отрицательное обогащение. *FDR < 0,05, **FDR < 0,01, ***FDR < 0,001 - статистическая значимость..

The most significant positive enrichment was found for the «TNFα signaling via NF-κB pathway» (NES = 2.69, FDR = 4.7×10^{-21}). Significant positive enrichment was also observed for the «IL6/JAK/STAT3 signaling» pathway (NES = 1.91, FDR = 1.3×10^{-3}). These results indicate that the NF-κB/IL6/JAK/STAT3 axis represents a prominent transcriptomic feature of PC3 cells surviving and recovering after stepwise DTX selection. Negative enrichment of proliferation- and mitotic cycle-related pathways was also observed in the experimental cells. Specifically, the «G2/M checkpoint» (NES = -1.49, FDR = 4.6×10^{-3}), «E2F targets» (NES = -1.51, FDR = 4×10^{-3}), «mitotic spindle» (NES = -1.54, FDR = 4×10^{-3}), and «protein secretion» (NES = -1.7, FDR = 4×10^{-3}) pathways were negatively enriched. These results demonstrate suppression of proliferative and mitotic programs, which is consistent with the mechanism of DTX action as a chemotherapeutic taxane that disrupts microtubule dynamics and mitotic cell division.

Figure 2. Heatmap analysis of selected leading-edge genes from significantly enriched Hallmark in DTX-selected PC3 cells

Рисунок 2. Анализ с помощью тепловой карты отдельных ведущих генов из значимых обогащённых Hallmark сигнатур в DTX-отобранных клетках PC3

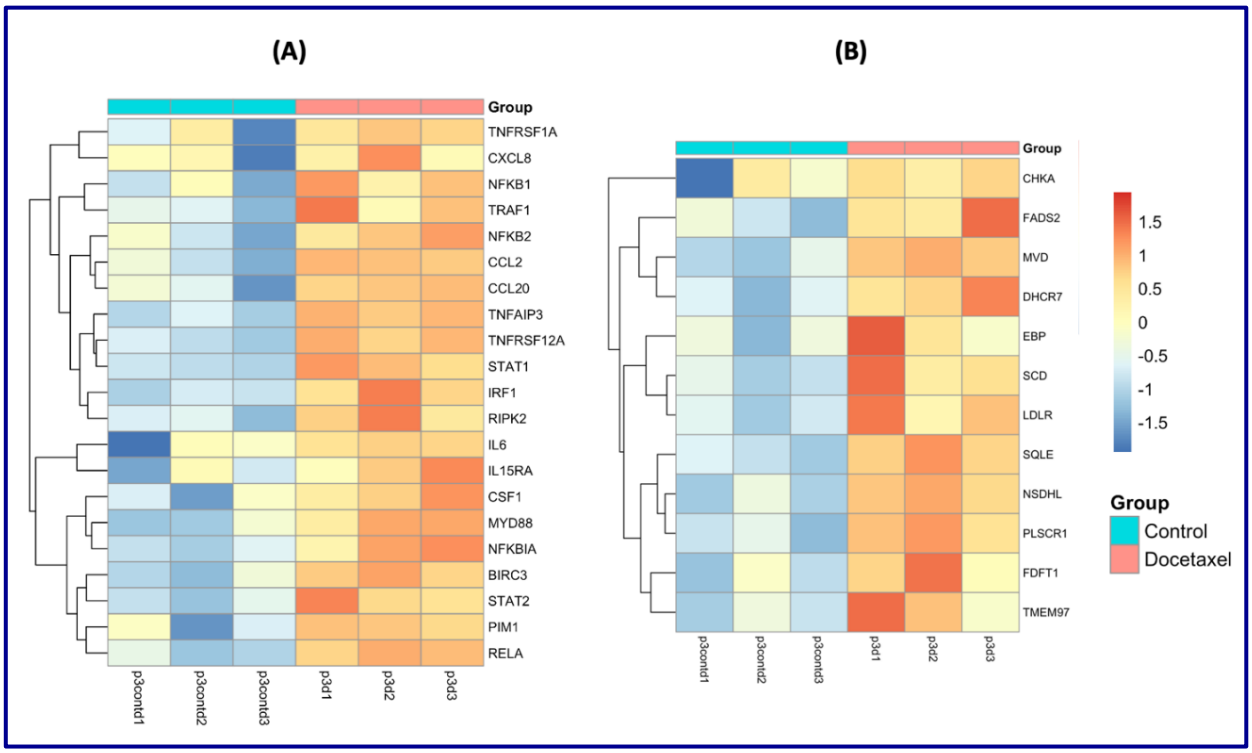

Note. (A) Selected leading-edge genes associated with the NF-κB/IL6/JAK/STAT3-related signature. (B) Selected leading-edge genes from the Hallmark cholesterol homeostasis signature. Expression values were scaled by gene and are presented as row z-scores. Cell colors indicate the relative expression level of each gene across samples: blue corresponds to expression below the gene-specific mean, yellow to intermediate expression, and orange to expression above the gene-specific mean.

Примечание. (A) Отдельные ведущие гены, связанные с сигнатурой NF-κB/IL6/JAK/STAT3. (B) Отдельные ведущие гены из Hallmark сигнатуры «гомеостаз холестерина». Значения экспрессии были нормированы по гену и представлены в виде z-показателей по строкам. Цвета ячеек отражают относительный уровень экспрессии каждого гена в образцах: синий цвет соответствует экспрессии ниже среднего значения для данного гена, жёлтый - промежуточной экспрессии, а оранжевый - экспрессии выше среднего значения для данного гена.

To further evaluate the NF-κB/IL6/JAK/STAT3-associated inflammatory-stress signature, a heatmap of selected leading-edge genes was constructed (fig. 2A). The selected genes included: *IL6, TNFRSF1A, TNFRSF12A, RELA, NFKB1, NFKB2, NFKBIA, NFKBIE, TNFAIP3, CCL2, CCL20, CXCL8, CSF1, RIPK2, MYD88, TRAF1, BIRC3*, and *PIM1*. Most of these genes showed higher VST-normalized expression values in DTX-selected cells compared to control samples. Together, these data support the presence of an inflammatory-stress transcriptional signature consistent with NF-κB/IL6/JAK/STAT3-associated signaling in DTX-selected cells. Also of particular interest was the enrichment of the «Cholesterol homeostasis» pathway (NES = 2.12; FDR = 6×10^{-6}) in DTX-selected PC3 cells. To visualize this metabolic signature, a heatmap of selected leading-edge genes from the Hallmark cholesterol homeostasis gene set was constructed (Fig. 2B). The genes included: *MVD, NSDHL, SQLE, FDFT1, LDLR, DHCR7, EBP, FADS2, TMEM97, SCD, CHKA*, and *PLSCR*. These genes are involved in sterol/cholesterol biosynthesis, uptake, and lipid metabolism. This concerted change likely reflects a rewiring of the cholesterol-associated metabolic program, which may be related to cellular adaptation to stepwise DTX selection.

To assess whether the identified PC3-associated transcriptomic signatures are reproducible at the pathway level, we additionally analyzed two independent public RNA-seq datasets of PC3 cells after DTX treatment, GSE233647 and GSE140440. Comparison of significantly enriched Hallmark signatures revealed five pathways shared across all three datasets: TNFα signaling via NF-κB, hypoxia, inflammatory response, complement, and epithelial–mesenchymal transition (fig. 3, table 2).

Figure 3. External in silico assessment of pathway-level concordance between the PC3 datasets

Рисунок 3. Внешняя in silico оценка согласованности на уровне сигнальных путей между PC3 наборами данных

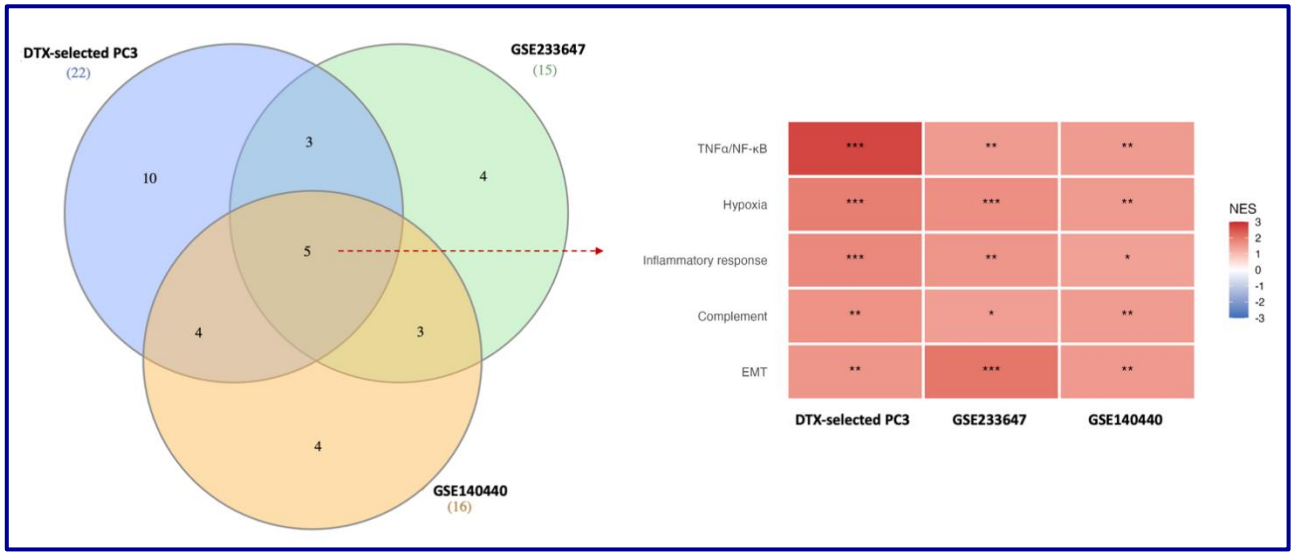

Note. The Venn diagram shows the overlap of significantly enriched Hallmark signatures among the three datasets. The heatmap shows the normalized enrichment score (NES) for these common pathways. Red indicates positive enrichment, whereas blue indicates negative enrichment. *FDR < 0.05, **FDR < 0.01, ***FDR < 0.001 - statistical significance.

Примечание. Диаграмма Венна показывает перекрытие значимо обогащённых Hallmark сигнатур между тремя наборами данных. Тепловая карта показывает нормализованный показатель обогащения (NES) для этих общих путей. Красный цвет указывает на положительное обогащение, тогда как синий цвет указывает на отрицательное обогащение. *FDR < 0,05, **FDR < 0,01, ***FDR < 0,001 - статистическая значимость.

All five signatures demonstrated concordant positive enrichment across all datasets, supporting the reproducibility of inflammatory/stress-associated transcriptional remodeling in PC3 cells under DTX-associated selective pressure.

Table 2. Concordantly enriched Hallmark signatures in the DTX-selected PC3 dataset and two independent public PC3 datasets

Таблица 2. Согласованно обогащённые Hallmark сигнатуры в наборе данных DTX-отобранных клеток PC3 и двух независимых общедоступных PC3 наборах данных

Pathway	DTX-selected PC3		GSE233647		GSE140440	
	NES	FDR	NES	FDR	NES	FDR
TNFα signaling via NF-κB	2.69	4.70×10^{-21}	1.50	8.10×10^{-3}	1.50	3.50×10^{-3}
Hypoxia	1.91	1.79×10^{-5}	1.67	9.70×10^{-4}	1.50	3.50×10^{-3}
Inflammatory response	1.76	5.93×10^{-4}	1.57	8.10×10^{-3}	1.39	2.50×10^{-2}
Complement	1.62	2.79×10^{-3}	1.44	2.40×10^{-2}	1.48	4.40×10^{-3}
Epithelial-mesenchymal transition	1.57	3.96×10^{-3}	2.05	5.70×10^{-7}	1.53	2.60×10^{-3}

Note. NES, normalized enrichment score; FDR, false discovery rate. Positive NES values indicate enrichment in DTX-selected PC3 cells, whereas negative NES values indicate negative enrichment relative to control PC3 cells.

Примечание. NES - нормализованный показатель обогащения; FDR - частота ложноположительных результатов. Положительные значения NES указывают на обогащение в DTX-отобранных клетках PC3, тогда как отрицательные значения NES указывают на отрицательное обогащение относительно контрольных клеток PC3.

DISCUSSION

One of the main findings of this study was the identification of an inflammatory/stress-associated transcriptomic signature in DTX-selected PC3 cells. At the GSEA level, this program was represented by a consistent positive enrichment of the TNFα signaling via NF-κB, inflammatory response, and IL6/JAK/STAT3 signaling pathways. The most pronounced signal was observed for the TNFα/NF-κB signature, suggesting activation of an NF-κB-associated transcriptional program in PC3

cells surviving and recovering after stepwise DTX selection. These findings should be interpreted as pathway-level transcriptomic associations rather than direct evidence of a causal role of NF-κB/IL6/JAK/STAT3 signaling in DTX resistance. Various studies have previously shown an association between NF-κB/IL6 signaling and the response to DTX and the development of a resistant phenotype in PCa models. Subsequent studies have also demonstrated the involvement of the NF-κB–IL6–STAT3 axis in PCa progression and DTX chemoresistance. Furthermore, inhibition of NF-κB-STAT3 dependent programs can enhance the effect of DTX, highlighting the potential for targeting this axis [Codony-Servat *et al.* 2013; Zhong *et al.* 2022; Cruz-Lozano *et al.* 2024].

The relevance of the inflammatory/stress-associated remodeling was further supported by an external *in silico* analysis of two independent public PC3 RNA-seq datasets, GSE233647 and GSE140440. Across the DTX-selected PC3 dataset and both public PC3 datasets, five Hallmark signatures showed concordant positive enrichment: TNFα signaling via NF-κB, hypoxia, inflammatory response, complement, and epithelial–mesenchymal transition. This overlap supports the reproducibility of a broader inflammatory/stress-related transcriptional state in PC3 cells under DTX-associated selective pressure. Importantly, the public dataset analysis was used to assess pathway-level concordance and should not be interpreted as direct functional validation of DTX resistance.

The IL6/JAK/STAT3-associated axis emphasizes the search for secondary fungal metabolites with anti-inflammatory signaling activity. Such compounds may include metabolites of various structural groups - lactone derivatives, triterpenoids, polyketides, alkaloids, and other compounds, whose antitumor effects may be linked to the regulation of key tumor-associated signaling cascades [Evidente 2024]. The best characterized compound is galiellalactone, a secondary metabolite with documented STAT3-inhibitory activity, first isolated from the ascomycete *Galiella rufa* strain A111-95 [Köpcke *et al.* 2002]. This metabolite has been characterized as a direct STAT3 inhibitor, and galiellalactone has also been shown to inhibit the growth of STAT3-activated cells *in vitro* and *in vivo* in PCa models [Don-Doncow *et al.* 2014; Thaper *et al.* 2018]. It is worth noting that galiellalactone activity has also been demonstrated in other cancer types, such as in a breast cancer model where analogs capable of inhibiting STAT3 phosphorylation and inducing apoptosis in tumor cells were developed based on the structure of natural galiellalactone [Ko *et al.* 2019]. These results indicate the possibility of further chemical optimization of this compound for further studies.

Triterpenoids, particularly ganoderic acids produced by fungi of the genus *Ganoderma*, including *Ganoderma lucidum*, may be of interest as an additional direction for exploring fungal secondary metabolites capable of modulating the NF-κB/IL6/JAK/STAT3 axis. Proapoptotic, cytotoxic, and anti-invasive effects have been described for this class of compounds in tumor models [García-Estrada *et al.* 2025].

The cholesterol-associated metabolic program emerged as another transcriptomic signature relevant to the subsequent selection of fungal metabolite classes. In our data, cholesterol homeostasis was positively enriched, and this enrichment was also observed in GSE140440 public PC3 dataset (NES = 1.52, FDR = 0.018), suggesting that cholesterol-associated remodeling may represent a reproducible but context-dependent component of the PC3 adaptive response. The biological significance of cholesterol metabolism is consistent with studies on the role of lipid metabolism in PCa progression, which indicate that dysregulation of lipid and cholesterol metabolism may serve as a tumor cell survival strategy and a potential therapeutic vulnerability [Guerrero-Ochoa *et al.* 2024]. In addition, remodeling of fatty acid, cholesterol, and phospholipid metabolism has been described as one of the key features of tumor progression and metabolic adaptation [Zhang *et al.* 2023].

Given the enrichment of cholesterol homeostasis in DTX-selected PC3 cells, statin-like fungal metabolites can be considered one of the promising classes of compounds for further screening of potential modifiers of drug tolerance [Tripathi *et al.* 2024]. Fungal statin-like metabolites, such as lovastatin produced by *Aspergillus terreus* and *Monascus sp.* and compactin/mevastatin produced by *Penicillium sp.*, may be considered for future screening. Moreover, lovastatin has been shown to exhibit antitumor effects through the induction of apoptosis, suppression of proliferation, inhibition of angiogenesis, and potential enhancement of tumor cell sensitivity to chemotherapeutic drugs [García-Estrada *et al.* 2025]. Thus, this class of fungal secondary metabolites can be considered a promising pool of compounds for subsequent screening of drug tolerance modifiers. It is important to note that the cholesterol-associated program should be considered a second, metabolically oriented direction for experimental targeting, complementing the central NF-κB/IL6/JAK/STAT3-associated axis.

Overall, our results suggest that PC3 cells surviving and recovering after stepwise DTX selection are characterized by adaptive changes in inflammatory and metabolic transcriptomic programs. The identified NF-κB/IL6/JAK/STAT3- and cholesterol homeostasis-associated signatures may serve as reference points for subsequent targeted searches for candidate compounds potentially capable of modulating DTX-associated adaptive programs in tumor cells. However, several limitations of this study should be considered, including the use of a single PC3-based model, which limits the generalizability of the findings to other PCa cell lines with different molecular backgrounds, such as DU145 or LNCaP, and the lack of validation of the identified pathways at the protein and functional levels. Finally, the fungal secondary metabolites discussed here were selected based on literature data and were not tested experimentally in this model. Therefore, they should be considered candidate compounds for future experimental validation.

FINANCIAL SUPPORT | ФИНАНСОВАЯ ПОДДЕРЖКА

This work was financially supported by the Russian Science Foundation, grant 25-24-01217.

Conflicts of Interest | Конфликт интересов

The authors declare no actual or potential conflicts of interest related to the publication of this article.

REFERENCES

Bills G.F., Gloer J.B. (**2016**) Biologically Active Secondary Metabolites from the Fungi. *Microbiology Spectrum*. **4**(6) https://doi.org/10.1128/microbiolspec.FUNK-0009-2016

Candia J., Ferrucci L. (**2024**) Assessment of Gene Set Enrichment Analysis using curated RNA-seq-based benchmarks. *PloS One*. **19**(5): e0302696. https://doi.org/10.1371/journal.pone.0302696 EDN: WXMAVI

Codony-Servat J., Marín-Aguilera M., Visa L., García-Albéniz X., Pineda E., Fernández P.L., Filella X., Gascón P., Mellado B. (**2013**) Nuclear factor-kappa B and interleukin-6 related docetaxel resistance in castration-resistant prostate cancer. *The Prostate*. **73**(5): 512–521. https://doi.org/10.1002/pros.22591

Cruz-Lozano J.R., Hernández-Flores G., Ortiz-Lazareno P.C., Palafox-Mariscal L.A., Vázquez-Ibarra K.C., González-Martínez K.L., Villaseñor-García M.M., Bravo-Cuellar A. (**2024**) Improvement of Docetaxel Efficacy through Simultaneous Blockade of Transcription Factors NF-κB and STAT-3 Using Pentoxifylline and Stattic in Prostate Cancer Cells. *Current Issues in Molecular Biology*. **46**(9): 10140–10159. https://doi.org/10.3390/cimb46090605 EDN: ARLBOY

Dhiman V.K., Kumari M., Singh D. (**2026**) Chemoresistance: The hidden barrier in cancer treatment. *Cancer Pathogenesis and Therapy*. **4**(2): 98–109. https://doi.org/10.1016/j.cpt.2025.07.001 EDN: ENZRJL

Don-Doncow N., Escobar Z., Johansson M., Kjellström S., Garcia V., Munoz E., Sterner O., Bjartell A., Hellsten R. (**2014**) Galiellalactone is a direct inhibitor of the transcription factor STAT3 in prostate cancer cells. *The Journal of Biological Chemistry*. **289**(23): 15969–15978. https://doi.org/10.1074/jbc.M114.564252

Ergin S., Kherad N., Alagoz M. (**2022**) RNA sequencing and its applications in cancer and rare diseases. *Molecular Biology Reports*. **49**(3): 2325–2333. https://doi.org/10.1007/s11033-021-06963-0 EDN: NJOMCK

Evidente A. (**2024**) Advances on anticancer fungal metabolites: sources, chemical and biological activities in the last decade (2012-2023). *Natural Products and Bioprospecting*. **14**(1): 31. https://doi.org/10.1007/s13659-024-00452-0 EDN: KBIIXM

García-Estrada C., Barreiro C., Martín J.F. (**2025**) Anticancer Secondary Metabolites Produced by Fungi: Potential and Representative Compounds. *International Journal of Molecular Sciences*. **27**(1): 101. https://doi.org/10.3390/ijms27010101 EDN: KNCJYK

Gu Y., Yang R., Zhang Y., Guo M., Takehiro K., Zhan M., Yang L., Wang H. (**2025**) Molecular mechanisms and therapeutic strategies in overcoming chemotherapy resistance in cancer. *Molecular Biomedicine*. **6**(1): 2. https://doi.org/10.1186/s43556-024-00239-2 EDN: VIQHEJ

Guerrero-Ochoa P., Rodríguez-Zapater S., Anel A., Esteban L.M., Camón-Fernández A., Espilez-Ortiz R., Gil-Sanz M.J., Borque-Fernando Á. (**2024**) Prostate Cancer and the Mevalonate Pathway. *International Journal of Molecular Sciences*. **25**(4): 2152. https://doi.org/10.3390/ijms25042152 EDN: VYHOZP

Hussain M., Fizazi K., Shore N.D., Heidegger I., Smith M.R., Tombal B., Saad F. (**2024**) Metastatic Hormone-Sensitive Prostate Cancer and Combination Treatment Outcomes: A Review. *JAMA Oncology*. **10**(6): 807. https://doi.org/10.1001/jamaoncol.2024.0591 EDN: ZXOZHM

Ko H., Lee J., Kim H., Kim T., Han Y., Suh Y.-G., Chun J., Kim Y., Ahn K. (**2019**) Novel Galiellalactone Analogues Can Target STAT3 Phosphorylation and Cause Apoptosis in Triple-Negative Breast Cancer. *Biomolecules*. **9**(5): 170. https://doi.org/10.3390/biom9050170 EDN: KKWWNS

Köpcke B., Weber R.W.S., Anke H. (**2002**) Galiellalactone and its biogenetic precursors as chemotaxonomic markers of the Sarcosomataceae (Ascomycota). *Phytochemistry*. **60**(7): 709–714. https://doi.org/10.1016/S0031-9422(02)00193-0 EDN: AYCYGD

Le T.K., Duong Q.H., Baylot V., Fargette C., Baboudjian M., Colleaux L., Taïeb D., Rocchi P. (**2023**) Castration-Resistant Prostate Cancer: From Uncovered Resistance Mechanisms to Current Treatments. *Cancers*. **15**(20): 5047. https://doi.org/10.3390/cancers15205047 EDN: YMLWYS

Menyhart O., Kothalawala W.J., Győrffy B. (**2025**) A gene set enrichment analysis for cancer hallmarks. *Journal of Pharmaceutical Analysis*. **15**(5): 101065. https://doi.org/10.1016/j.jpha.2024.101065 EDN: QVPJXK

Pudova E., Kobelyatskaya A., Katunina I., Snezhkina A., Nyushko K., Fedorova M., Pavlov V., Bulavkina E., Dalina A., Tkachev S. *et al.* (**2022**) Docetaxel Resistance in Castration-Resistant Prostate Cancer: Transcriptomic Determinants and the Effect of Inhibiting Wnt/β-Catenin Signaling by XAV939. *International Journal of Molecular Sciences*. **23**(21): 12837. https://doi.org/10.3390/ijms232112837 EDN: CPGQLC

Sekino Y., Teishima J. (**2020**) Molecular mechanisms of docetaxel resistance in prostate cancer. *Cancer Drug Resistance*. https://doi.org/10.20517/cdr.2020.37 EDN: GIONCE

Siegel R.L., Kratzer T.B., Giaquinto A.N., Sung H., Jemal A. (**2025**) Cancer statistics, 2025. *CA: A Cancer Journal for Clinicians*. **75**(1): 10–45. https://doi.org/10.3322/caac.21871 EDN: MHQXTB

Sonowal S., Gogoi U., Buragohain K., Nath R. (**2024**) Endophytic fungi as a potential source of anti-cancer drug. *Archives of Microbiology*. **206**(3): 122. https://doi.org/10.1007/s00203-024-03829-4 EDN: FYOTSP

Thaper D., Vahid S., Kaur R., Kumar S., Nouruzi S., Bishop J.L., Johansson M., Zoubeidi A. (**2018**) Galiellalactone inhibits the STAT3/AR signaling axis and suppresses Enzalutamide-resistant Prostate Cancer. *Scientific Reports*. **8**(1): 17307. https://doi.org/10.1038/s41598-018-35612-z EDN: ODCBXT

Tripathi S., Gupta E., Galande S. (**2024**) Statins as anti-tumor agents: A paradigm for repurposed drugs. *Cancer Reports*. **7**(5): e2078. https://doi.org/10.1002/cnr2.2078 EDN: XJKYLE

Zafar A., Khatoon S., Khan M.J., Abu J., Naeem A. (**2025**) Advancements and limitations in traditional anti-cancer therapies: a comprehensive review of surgery, chemotherapy,

radiation therapy, and hormonal therapy. *Discover Oncology*. **16**(1): 607. https://doi.org/10.1007/s12672-025-02198-8 EDN: GYFUQZ

Zhang S., Shi G., Xu X., Guo X., Li S., Li Z., Wu Q., Yin W.-B. (**2024**) Global Analysis of Natural Products Biosynthetic Diversity Encoded in Fungal Genomes. *Journal of Fungi*. **10**(9): 653. https://doi.org/10.3390/jof10090653 EDN: XQUNQQ

Zhang Z., Wang W., Kong P., Feng K., Liu C., Sun T., Sang Y., Duan X., Tao Z., Liu W. (**2023**) New insights into lipid metabolism and prostate cancer (Review). *International Journal of Oncology*. **62**(6): 74. https://doi.org/10.3892/ijo.2023.5522 EDN: EXURLP

Zhong W., Wu K., Long Z., Zhou X., Zhong C., Wang S., Lai H., Guo Y., Lv D., Lu J. *et al.* (**2022**) Gut dysbiosis promotes prostate cancer progression and docetaxel resistance via activating NF-κB-IL6-STAT3 axis. *Microbiome*. **10**(1): 94. https://doi.org/10.1186/s40168-022-01289-w EDN: LSXQUU

Cited as

Katunina I.V., Shishkina A.S., Pudova E.A. (**2026**). Transcriptomic signatures of docetaxeladaptation in the PC3 prostate cancer cell line: NF-κB/IL6/JAK/STAT3-signaling and cholesterol metabolism as guides for the search for fungal secondary metabolites. *Ecobiotech*. **9**(2): 209-219. DOI: http://doi.org/10.31163/2618-964X/2026-17
EDN: https://www.elibrary.ru/nmqllk

Цитировать как

Катунина И.В., Шишкина А.С., Пудова Е.А. (**2026**). Транскриптомные сигнатуры адаптации к доцетакселу в клеточной линии рака предстательной железы PC3: NF-κB/IL6/JAK/STAT3-сигналинг и метаболизм холестерина как ориентиры для поиска вторичных метаболитов грибов. *Экобиотех*. **9**(2): 209-219.
DOI: http://doi.org/10.31163/2618-964X/2026-17
EDN: https://www.elibrary.ru/nmqllk

Information About the Author(s)

Irina Vasilievna Katunina, Engelhardt Institute of Molecular Biology, Russian Academy of Sciences, Moscow, Russia. E-mail: i.katunina125@gmail.com, WoS ResearcherID: OUI-4906-2025, Scopus ID: 57751657100, ORCID: 0009-0008-8106-2487.

Anna Sergeevna Shishkina, Engelhardt Institute of Molecular Biology, Russian Academy of Sciences, Moscow, Russia. E-mail: Shishkinaanna2020@mail.ru

Elena Anatolevna Pudova, PhD in Biological Sciences, Engelhardt Institute of Molecular Biology, Russian Academy of Sciences, Moscow, Russia. E-mail: pudova_elena@inbox.ru, SPIN-код: 6520-5505, WoS ResearcherID: P-9299-2017, Scopus ID: 57194144947, ORCID: 0000-0002-5492-1361.

Сведения об авторе/ах

Ирина Васильевна Катунина, Институт молекулярной биологии им. В.А. Энгельгардта РАН, Москва, Россия. E-mail: i.katunina125@gmail.com, WoS ResearcherID: OUI-4906-2025, Scopus ID: 57751657100, ORCID: 0009-0008-8106-2487.

Анна Сергеевна Шишкина, Институт молекулярной биологии им. В.А. Энгельгардта РАН, Москва, Россия. E-mail: Shishkinaanna2020@mail.ru

Елена Анатольевна Пудова, к.б.н, Институт молекулярной биологии им. В.А. Энгельгардта РАН, Москва, Россия. E-mail: pudova_elena@inbox.ru, SPIN-код: 6520-5505, WoS ResearcherID: P-9299-2017, Scopus ID: 57194144947, ORCID: 0000-0002-5492-1361.

LIST OF ABBREVIATIONS

AR - Androgen receptor
CRPC - Castration-resistant prostate cancer
E2F - E2 transcription factor family
FBS - Fetal bovine serum
FDR - False discovery rate
FASTQ - sequencing data format
G2/M - Gap 2/mitosis phase of the cell cycle
GSEA - Gene Set Enrichment Analysis
IL6 - Interleukin 6
JAK - Janus kinase
mRNA - Messenger RNA
NES - Normalized enrichment score
NF-κB - Nuclear factor kappa-light-chain-enhancer of activated B cells
PCa - Prostate cancer
PC3 - Human prostate cancer cell line PC-3
RNA-seq - RNA sequencing
STAT3 - Signal transducer and activator of transcription 3
TNFα - Tumor necrosis factor alpha
VST - Variance-stabilizing transformation